

A high-sensitivity biosensor based on metal–insulator–metal and rectangular resonator for biochemical detection

Hocine Bahri

Laboratory of Electronics and New Technologies (LENT),
University Oum El Bouaghi, Algeria
bahri.hocine@univ-oeb.dz

Souheil Mouetsi

Laboratory of Electronics and New Technologies (LENT), University Oum El Bouaghi, Algeria
s.mouetsi@univ-oeb.dz

Abdssalam Hocini

Laboratoire d'Analyse des Signaux et Systèmes, Département of Electronics
Univers- city of M'Sila, BP.166, Route Ichebilia, M'sila, 28000 Algeria

Sven Ingebrandt

Institute of Materials in Electrical Engineering 1, RWTH Aachen University, Sommerfeldstraße 24, D-52074 Aachen, Germany
ingebrandt@iwe1.rwth-aachen.de

Vivek Pachauri

Institute of Materials in Electrical Engineering 1, RWTH Aachen University, Sommerfeldstraße 24, D-52074 Aachen, Germany
pachauri@iwe1.rwth-aachen.de

Hocine Ben Slah

Laboratoire d'Analyse des Signaux et Systèmes, Département of Electronics
Univers- city of M'Sila, BP.166, Rou Ichebilia, M'sila, 28000 Algeria
University yahia fares médéa, Algeria

Abstract—Herein, a refractive index sensing based on a novel design of rectangular cavity couple with defect nanorod (RCDN), using metal-insulator-metal (MIM) waveguide is suggested for biochemical application. Herein, the optimized cavity design can provide the best sensing performance. In this work, we have numerically simulated with Finite-Difference-Time-Domain (FDTD) method, by varying small change in the geometric parameter we can bring a significant shift in the sensitivity of the device, also we can manipulate the resonance wavelength. The high sensitivity of the biosensor is 2035 nm/RIU. This device can be utilized in the on-chip detection of biochemical such glucose in water and cancer cells with high sensitivity.

Keywords— Refractive Index (RI), Metal-insulator-metal (MIM), Near-infrared (NIR) and mid-infrared (MIR), Finite-Difference-Time-Domain (FDTD), biosensor

I. INTRODUCTION

Surface plasmon polaritons (SPPs) is an electromagnetic excitation that propagates along with the interface between a metal and a dielectric medium and whose amplitude decays exponentially with increasing distance into each medium from the interface[1]. Exhibit interesting and valuable properties such as energy asymptote in dispersion curves, resonant modes, field localization and enhancement, high sensitivity, and subwavelength confinement[2]. potential properties of SPPs are acknowledged to have a fast (rapid response), cost-effective, low-regent-consumption, easy-of-use (label-free), SPPs have the ability to field confinement, focus and channel light in subwavelength scale metallic structure to increase the photo lifetime, which enhance the near field of light-mater leading to high sensitivities (surface and bulk) to the slight change of the refractive index (RI) by dictating the evanescent tail of the SPP. Therefore, the SPP has a potential in medical diagnostics and environmental monitoring as RNA[3], DNA[4], protein [5], viruses [6], glucose concentration[7].Furher, surface plasmon resonance (SPR) has the ability of a high degree of integration, miniaturization, overcoming the diffraction limits, and localization of light in subwavelength regions, SPR has attracted attention in the scientific community and studied experimentally and theoretically the potential to guide, concentrate, and scatter light at the nanoscale[8].

one of the interesting plasmonic structures as MIM metal-insulator-metal (MIM), has more transmission loss(it

can be neglected in nano-scale[9] and supports the propagation of SPP. Thus, was used for many fields as a sensors[10], filters[11], demultiplexers[12], switches[10], and splitters[13]. Over the past few years, a several unique cavity designs used to improve the sensing performance of the plasmonic sensors based on the MIM waveguide such a disk resonators [8], double cavities [10], hexagonal cavities [14], rectangular resonators [15], nanorods [16]. many researchers is trying to increasing the sensitivity and improving the transmission spectrum by choosing a unique and thoughtful structures dimensions based on previous research papers. As a result, the optical biosensor on-chip with a tiny and sharp geometric feature using a plasmonic waveguide has been explored extensively

In this paper, a design based on a rectangular cavity couple with defect nanorod (RCDN) investigated for plasmonic biosensor using the Finite-Difference-Time-Domain (FDTD) method. The interaction of the RCDN create the transmission peaks. By varying the geometric parameters of the structure we control and manipulate the resonance wavelengths. Further We investigated this proposed sensor into sensing for different diseases, by using their unique refractive indices. Thus, the resonance wavelength is shifting, and this information allows us to calculate the sensitivity. The resonance wavelength increases almost linearly with RI content. Our proposed sensor can provide a sensitivity of 2035 nm/RIU with wavelength resolution reaching 3.84×10^{-6} RIU⁻¹, which can help discover broad applications in the plasmonics Nano sensing domain.

II. THEORY AND SIMULATION

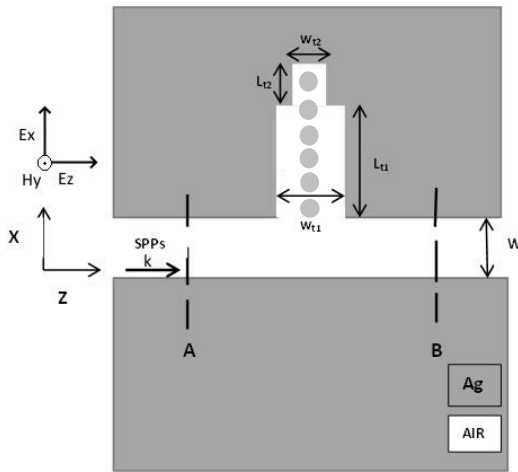


Fig 1(a) a MIM waveguide structure are illustrated

In Fig 1(a) a MIM waveguide structure are illustrated, which proposed a highly refractive index RI sensor composed of a straight waveguide couple with a ring of racetrack cavity and circular defect (hereafter represented as RRCCD). the device performance is compared with a other sensor design cavity and the RSOFT CAD software is used to calculate the transmission characteristics. Using a waveguide width as $W = 50\text{nm}$ coupled. All the structure parameters $D = 35\text{nm}$, $r = 15\text{nm}$, $Lt_1 = 175\text{nm}$, $Lt_2 = 75\text{nm}$, $Wt_1 = 50\text{nm}$ and $Wt_2 = 30\text{nm}$.

Furthermore, a detects incident light from the source and B detects received light at the waveguide's output to detect transmittance as $T = A/B$, the input light waves emitted from A partly reflected, partly coupled into DRT, and then transmitted out along the power monitors' output B. The silver layer and the dielectric (air) material are represented by the gray and white areas, respectively. By trapping incident light waves, the use of Ag as a metal in the MIM structure improves absorption. As a result, more SPRs are generated with the smallest damping constant, which is the best performing choice at optical frequency. Furthermore, the Ag provides a framework in which the fluid test substance can be used. The Drude-

Lorentz model gives the designated channel, The relative dielectric constant of silver [17]:

$$\epsilon_m = \epsilon_\infty - \frac{\omega_p^2}{\omega^2 - i\omega\gamma'} \quad (1)$$

Here, ϵ_∞ , γ , and ω_p are the dielectric constant at the infinite frequency, the electron collision frequency, the bulk plasma frequency, respectively. The parameters

are set to be $\epsilon_\infty = 3.7$, $\omega_p = 9.1 \text{ eV}$, $\gamma = 0.018 \text{ eV}$. During the FDTD simulations since the wavelength of the incident light is greater than the waveguide's width, only a single propagation mode TM_0 can exist in the structure, The TM mode dispersion equation of this case can be described by [18]:

$$\epsilon_d \sqrt{n_{ef}^2 - \epsilon_m} + \epsilon_m \sqrt{n_{ef}^2 - \epsilon_d} \tanh\left(\frac{W\pi \sqrt{n_{ef}^2 - \epsilon_m}}{\lambda}\right) = 0 \quad (2)$$

where ϵ_d is the permittivity of the dielectric, ϵ_m is the permittivity of the metal, n_{ef} is the effective refractive index, W is the width of the straight waveguide and λ is the wavelength of the incident light. We get the frequency dependent ϵ_m from (1), and ϵ_d can be defined by $\epsilon_d = n^2$ where n is the refractive index of the dielectric. Therefore, A TM -polarized plane wave throws the MIM structure, the incident light will be coupled into the waveguide, and SPP waves are formed on the two metal interfaces. Ref19 gives the dispersion relation of the fundamental TM model in plasmonic waveguide structure, and the resonance wavelength of the ring resonator can be approximated by the following:

$$\lambda_m = \frac{2Re(\eta_{eff})L_{eff}}{m}, m=1,2,3.. \quad (3)$$

$Re(\eta_{eff})$ is the real part of the effective refractive index of the SPP, L_{eff} is the effective resonance length.

III. NUMERICAL RESULTS AND DISCUSSION

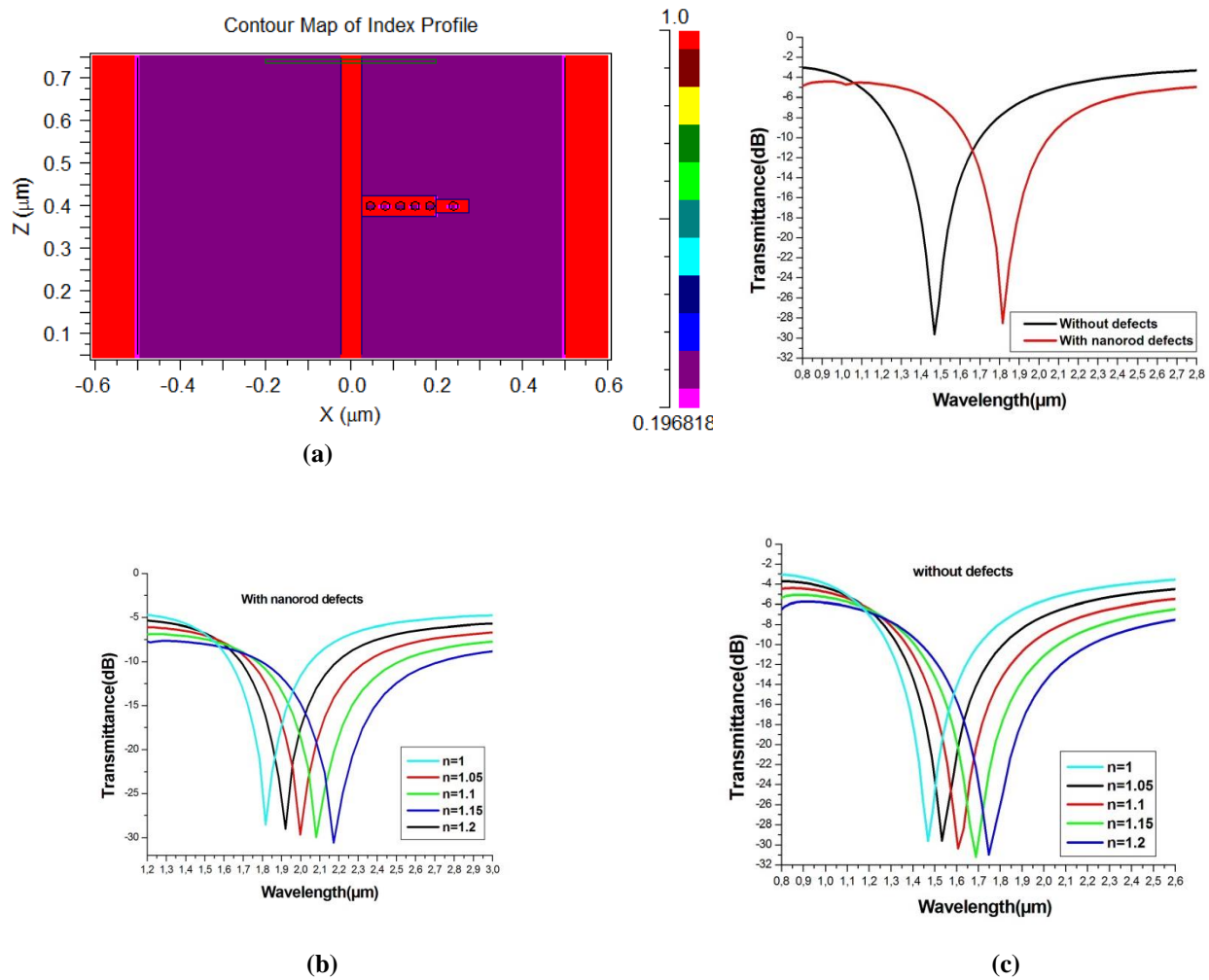


Fig 2. The MIM plasmonic structure with nanorod defects (a), Transmittance spectrum of the proposed plasmonic MIM waveguide (b) without defects and with metal nanorod defects. Transmittance spectra of the proposed MIM sensor (c) without and (d) with metal nanorod defects in cavity filled with different refractive index (RI) in the active region of the sensor and $D=35\text{nm}$, $r = 15\text{nm}$, $Lt_1=175\text{nm}$, $Lt_2=75\text{nm}$, $Wt_1=50\text{nm}$ and $Wt_2=30\text{nm}$.

A two-dimensional FDTD method is used, with the grid sizes in the x and z directions as $\Delta x = \Delta z = 3\text{nm}$, and the time step, derived by Courant condition is $\Delta t = 0.95 \frac{c}{\sqrt{(\Delta x)^2 + (\Delta z)^2}}$ to ensure that all the outside waves are emitted, we use a perfect match layer (PML) as an absorbing boundary condition for the computational window's boundaries. The first step, filling the insulator with nothing, means that the insulator is the air ($n=1$) as shown in Fig. 2(b), we achieve one sharp peak with high transmission at a wavelength without defects $\lambda_{res} = 1.4687 \mu\text{m}$, and with nanorod defects $\lambda_{res} = 1.8185 \mu\text{m}$. Next, In Fig. 2(c,d), the transmission spectrum has been studied versus the wavelength for different refractive index RI ranges from $n=1$ to 1.2 with a step of 0.05 for both structures, while the other parameters remain unchanged. In Fig. 2(d) the resonance wavelength shifts as we increase the RI, this redshift phenomenon due to the proportional

relationship between the $\text{Re}(n_{eff})$ and the wavelength λ according to Eq (2). a change in the resonant wavelength $\Delta\lambda$ provides information about the refractive index shift Δn . To this, it is common practice to establish the most essential characteristics to characterize its performance, with the values of these parameters recommended to be considerably higher for biosensor devices, such as the spectrum sensitivity of such sensors, defined as $S = \Delta\lambda/\Delta n$ [19]. For this structure, the sensitivity is $S(\text{without defect}) = 1398\text{nm}/\text{RIU}$, and $S(\text{defect nanorod}) = 2035\text{nm}/\text{RIU}$.

To get a better understanding of the mechanism of the inner magnetic field. Therefore, the Fig. 3 illustrate the magnetic field pattern of $|H_y|$ at the wavelength of the peak, as we can notice an intense energy distribution can be observed inside the cavities and nothing in the output waveguide, however, off the resonance wavelength of the peak, the robust energy can be observed in the output, which conforms with the result we obtained in Fig 2 (b).

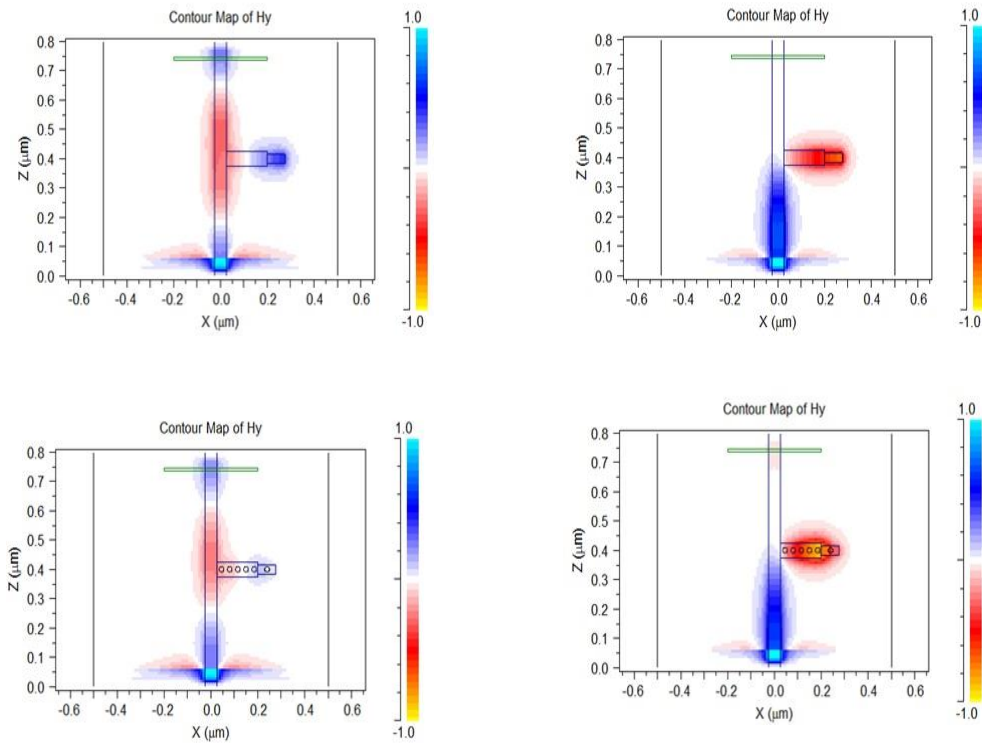


Fig. 3 Magnetic-field patterns of the MIM plasmonic structure without defects (at $\lambda = 1\mu\text{m}$ (a), $\lambda_{\text{res}} = 1.4687\mu\text{m}$ (b)) and with nanorod defects (at $\lambda = 1\mu\text{m}$ (c), $\lambda_{\text{res}} = 1.8185\mu\text{m}$ (d))

Second by varying the RI from 1 to 1.2 with a step of 0.05 we studied the resonance wavelengths versus the refractive index for different r as it show in Fig 4(b). due to the proportional relationship between the $\text{Re}(n_{\text{eff}})$ and the wavelength λ_m according to Eq (3).

we achieve a sensitivity as $S = 1402\text{nm}/\text{RIU}$ and for $r = 10\text{nm}$ and $r = 15\text{nm}$ we obtained a sensitivity reach to $S = 2392\text{nm}/\text{RIU}$ and $S = 2035\text{nm}/\text{RIU}$, respectively.

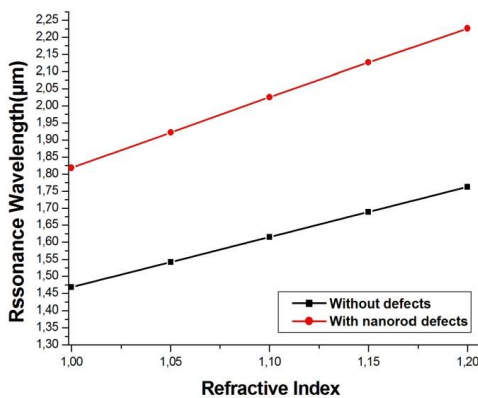


Fig. 4 Resonant wavelengths versus the refractive index (RI) without defects and with metal nanorod defects in cavity

We also carried out research on the performance of the geometry parameters to explain our choices for this structure. First, we studied the radius (r) of the circular cavity. To ensure the fabrication's feasibility, by varying r from 5 to 20 nm with a step of 5 nm, we noticed a shift occurring in the resonant peak, as shown in Fig 4 (a). Furthermore, as we increase the radius $r = 5\text{nm}$ in Fig 4 (c),

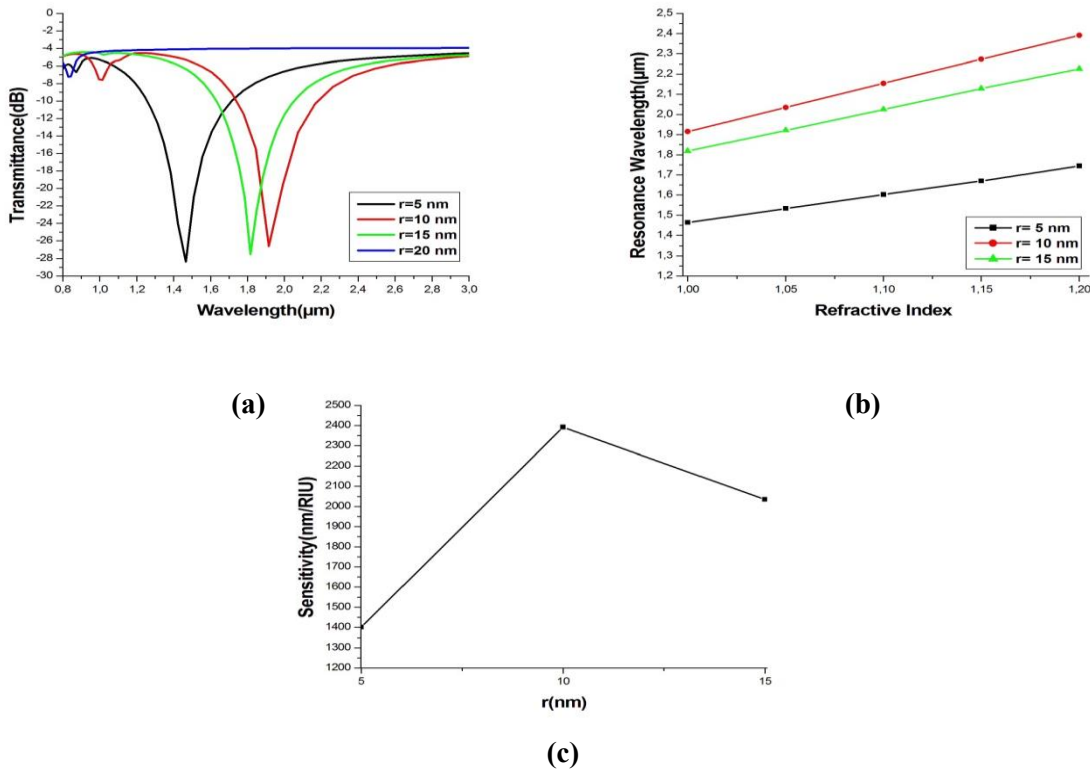


Fig. 5 Sensing properties as functions of r . (a) Transmission spectra of index 1 for r varying from 5 to 20 nm. (b) The resonance wavelengths versus the refractive index for different r . (c) Sensitivities of the plasmonic sensors for r varying from 0 to 15 nm.

IV. THE BIOMEDICAL APPLICATIONS OF THE PROPOSED PLASMONIC SENSOR

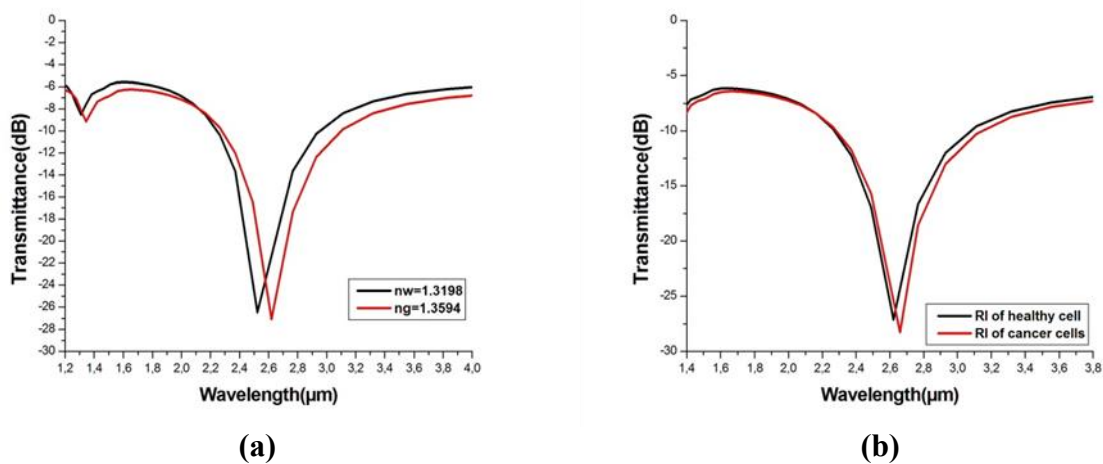


Fig. 6 (a) the peak of the transmission spectra versus the resonance wavelength for refractive index of the water $n_w = 1.3198$ and 25% solution of glucose in water as $n_g = 1.3594$. (b) The transmission spectrum versus the resonance wavelength for different refractive index of the cancer cells (1.37) and the healthy cells (1.353).

The following section use the sharper peak that occupies a narrower bandwidth in mid-IR from the previous result, as

illustrated in Fig. 6. The mid-IR range is particularly well-suited for biosensing as it encompasses the molecular

vibrations that uniquely identify the biochemical building blocks of life, such as proteins, lipids, and DNA[20]. In addition, engineered mid-IR substrates with extremely high field enhancements at distinct resonance wavelengths enable the ultrasensitive IR detection of small amounts of biomolecules.

The proposed plasmonic sensor in biomedical applications has been studied. Using a 25% glucose solution

in water alters the refractive index of water from $n_w = 1.3198$ to $n_g = 1.3594$, as Fig. 6(a) shows that we obtained a narrow, sharp peak with high transmission at the mid-IR range. A shift occurs as we change the RI of the surrounding medium, to study the RI of cancer[21] $n=1.370$, which is higher than the RI of the healthy cells (1.353) as depicted in Fig. 5(b), with a high sensitivity. All the results of the simulation have been summarized in Table 2.

Table. 2 Summary the result of the simulation

The test material	Refractive index	S (nm/RIU)
25% solution of glucose in water	$n_w = 1.3198,$ $n_g = 1.3594$	2315
Cancer cells	$n_1 = 1.353,$ $n_2 = 1.370$	2290

V. CONCLUSION

We have investigated a sample and new design of adjustable plasmonic nanostructures with high potential for biosensing applications in the near-IR and mid-IR bands. A rectangle and a defective Nanorod cavity are used in the proposed refractive index sensor. Furthermore, we investigated this structure for a variety of biological applications (detecting glucose, cancer, etc.). All the results of this structure show high sensitivities as 2035 nm/RIU and transmission spectra. This structure can pave the way for a plasmonic biosensor. This sensor has a large potential in biosensing and optical on-chip nano-sensors due to its high sensitivity, simple configuration, and compact structure; relatively easy fabrication, simple configuration, and compact structure.

REFERENCES

- [1] R. H. Ritchie, "Plasma losses by fast electrons in thin films Phys," *Phys. Rev.*, pp. 874–881, 1957.
- [2] P. Berini, "Loss Compensation and Amplification of Surface Plasmon Polaritons," *Act. Plasmon. Tuneable Plasmonic Metamaterials*, vol. 5, pp. 153–170, 2013.
- [3] X. Ding, Y. Yan, S. Li, Y. Zhang, and W. Cheng, "Analytica Chimica Acta Surface plasmon resonance biosensor for highly sensitive detection of microRNA based on DNA super-sandwich assemblies and streptavidin signal amplification," *Anal. Chim. Acta*, 2015, doi: 10.1016/j.aca.2015.03.021.
- [4] S. Filion-côté *et al.*, "Design and analysis of a spectro-angular surface plasmon resonance biosensor operating in the visible spectrum Design and analysis of a spectro-angular surface plasmon resonance biosensor operating in the visible spectrum," vol. 093107, 2014, doi: 10.1063/1.4894655.
- [5] G. T. Victor J. Hruby, "affinities Plasmon-waveguide resonance (PWR) spectroscopy for directly viewing rates of GPCR/G-protein interactions and quantifying affinities," vol. 7, no. 5, pp. 507–514, 2008.
- [6] M. Soler, X. Li, A. Belushkin, F. Yesilkoy, and H. Altug, "Towards a point-of-care nanoplasmonic biosensor for rapid and multiplexed detection of pathogenic infections," in *Plasmonics in Biology and Medicine XV*, 2018, vol. 10509, pp. 88–96, [Online]. Available: <https://doi.org/10.1117/12.2289752>.
- [7] A. H. E. Konstantinos Aidinis, Kiyanoush Goudarzi, "Optical sensor based on two-dimensional photonic crystals for measuring glucose in urine," *Opt. Eng.*, vol. 59, no. 5, p. 057104, 2020.
- [8] M. R. Rakhshani, A. Tavousi, and M. A. Mansouri-Birjandi, "Design of a plasmonic sensor based on a square array of nanorods and two slot cavities with a high figure of merit for glucose concentration monitoring," *Appl. Opt.*, vol. 57, no. 27, p. 7798, 2018, doi: 10.1364/ao.57.007798.
- [9] E. Han, Z. Liu, L. Forsberg, "Ultra-compact directional couplers and Mach-Zehnder interferometers employing surface plasmon polaritons," *Opt. Commun.*, vol. 25, pp. 690–69, 2006.
- [10] H. Ben salah, A. Hocini, M. N. Temmar, and D. Khedrouche, "Design of mid infrared high sensitive metal-insulator-metal plasmonic sensor," *Chinese J.*

- Phys.*, vol. 61, pp. 86–97, 2019, doi: 10.1016/j.cjph.2019.07.006.
- [11] A. Hocini, H. Ben salah, D. Khedrouche, and N. Melouki, “A high-sensitive sensor and band-stop filter based on intersected double ring resonators in metal–insulator–metal structure,” *Opt. Quantum Electron.*, vol. 52, no. 7, pp. 1–10, 2020, doi: 10.1007/s11082-020-02446-x.
- [12] Shiva Khani, Mohammad Danaie, Pejman Rezaei, “Double and triple-wavelength plasmonic demultiplexers based on improved circular nanodisk resonators,” *Opt. Eng.*, vol. 57, no. 10, p. 107102, 2018.
- [13] R. Negahdari, E. Rafiee, and F. Emami, “Realization of all-optical plasmonic MIM split square ring resonator switch,” *Opt. Quantum Electron.*, vol. 51, no. 7, 2019, doi: 10.1007/s11082-019-1924-7.
- [14] M. Nejat and N. Nozhat, “Multi-band MIM refractive index biosensor based on Ag-air grating with equivalent circuit and T-matrix methods in near-infrared region,” *Sci. Rep.*, vol. 10, no. 1, pp. 1–12, 2020, doi: 10.1038/s41598-020-63459-w.
- [15] M. Rahmatiyar and M. Afsahi, “Design of a Refractive Index Plasmonic Sensor Based on a Ring Resonator Coupled to a MIM Waveguide Containing Tapered Defects,” 2020.
- [16] C. T. C. Chao *et al.*, “Highly sensitive and tunable plasmonic sensor based on a nanoring resonator with silver nanorods,” *Nanomaterials*, vol. 10, no. 7, pp. 1–14, 2020, doi: 10.3390/nano10071399.
- [17] S. G. T.W. Lee, “Subwavelength light bending by metal slit structures,” *Opt. Express*, no. 13, pp. 9652–9659, 2015.
- [18] J. A. Dionne, L. A. Sweatlock, H. A. Atwater, and A. Polman, “Plasmon slot waveguides: Towards chip-scale propagation with subwavelength-scale localization,” *Phys. Rev. B - Condens. Matter Mater. Phys.*, vol. 73, no. 3, p. 035407, 2006, doi: 10.1103/PhysRevB.73.035407.
- [19] M. Reza and M. A. Mansouri-birjandi, “A high-sensitivity sensor based on three-dimensional metal – insulator – metal racetrack resonator and application for hemoglobin detection,” *Photonics Nanostructures - Fundam. Appl.*, vol. 32, no. January, pp. 28–34, 2018, doi: 10.1016/j.photonics.2018.08.002.
- [20] D. Rodrigo *et al.*, “Mid-infrared plasmonic biosensing with graphene,” *Science (80-.)*, vol. 349, no. 6244, pp. 165–168, 2015, doi: 10.1126/science.aab2051.
- [21] P. Y. Liu *et al.*, “Cell refractive index for cell biology and disease diagnosis: past, present and future,” *Lab Chip*, vol. 16, no. 4, pp. 634–644, 2016.